Activation of Pregnane X Receptor–Cytochrome P450s Axis: A Possible Reason for the Enhanced Accelerated Blood Clearance Phenomenon of PEGylated Liposomes In Vivo [S]

Fengling Wang,[1] Huihui Wang,[1] Yifan Wu, Lei Wang, Ling Zhang, Xi Ye, Daiyin Peng, and Weidong Chen

Institute of Drug Metabolism (F.W., H.W., Y.W., L.W., L.Z., D.P., W.C.) and Institute of Pharmaceutics (W.C.), School of Pharmaceutical Sciences, Anhui University of Chinese Medicine, Hefei, Anhui, China; Department of Pharmacy, The Second People's Hospital of Hefei, Hefei, Anhui, China (F.W., X.Y.); Anhui Province Key Laboratory of Chinese Medicinal Formula, Hefei, China (L.W., L.Z., D.P., W.C.); and Synergetic Innovation Center of Anhui Authentic Chinese Medicine Quality Improvement, Hefei, China (D.P., W.C.)

ABSTRACT

Recently, we reported that repeated injection of PEGylated liposomes (PEG-L) at certain intervals to the same rat lead to the disappearance of their long-circulation properties, referred to as the "accelerated blood clearance (ABC) phenomenon". Evidence from our recent studies suggested that cytochrome P450s (P450s) contribute to induction of the ABC phenomenon, a possibility that had been previously ignored. However, few details are known about the mechanism for induction of P450s. The present study was undertaken to investigate the roles in the ABC phenomenon of pregnane X receptor (PXR) and constitutive androstane receptor (CAR), the major upstream transcriptional regulators of the P450 genes, including CYP3A1, CYP2C6, and CYP1A2. The results demonstrated that expression of rat PXR and CAR was significantly increased in the ABC phenomenon and was accompanied by elevated CYP3A1, CYP2C6, and CYP1A2 levels. Further findings revealed that PXR but not CAR protein was substantially upregulated in the hepatocyte nucleus, together with marked nuclear colocalization of the PXR–retinoid X receptor alpha (RXRα) transcriptionally active heterodimer, indicating that nuclear translocation of PXR was induced in the ABC phenomenon, whereas nuclear translocation of CAR was not observed. Notably, pretreatment with the specific PXR inducer dexamethasone significantly induced accelerated systemic clearance of the subsequent injection of PEG-L, associating with increased nuclear colocalization of PXR-RXRα. These results revealed that the induction of P450s in the ABC phenomenon may be attributable largely to the activation of PXR induced by sequential injections of PEG-L, thus confirming the crucial involvement of the PXR-P450s axis in promoting the ABC phenomenon.

SIGNIFICANCE STATEMENT

The results of this study revealed that the induction of P450s in the ABC phenomenon may be largely attributable to the activation of PXR induced by sequential injections of PEG-L, thus confirming the crucial involvement of the PXR-P450s axis in promoting the ABC phenomenon. The data may help to extend our insights into 1) the role of P450s, which are regulated by the liver-enriched nuclear receptor PXR, in the ABC phenomenon, and 2) the therapeutic potential of targeting the PXR-P450 axis for reducing the magnitude of the ABC phenomenon in clinical practice.

Introduction

Polyethylene glycol (PEG) has been approved by Food and Drug Administration (FDA) as a safe hydrophilic polymer for modifying liposomes as a result of its prolonged circulation properties

(Suk et al., 2016). Recent evidence suggests that repeated injection of PEGylated liposomes (PEG-L), either empty vesicles or drug-containing vesicles, abolished the long circulation time and accelerated the elimination of liposomes from blood, which is referred to as the "accelerated blood clearance phenomenon" (Papahadjopoulos et al., 1991; Ishida and Kiwada, 2008; Li et al., 2015). Because many liposomal formulations require more than two injections for effective clinical application, this issue has become one of the foremost challenges for the translation of PEG-L into clinical research and applications. Using the anticancer agent docetaxel (DTX) as a model drug, we recently reported that intravenous injection of the long-circulating PEG-modified docetaxel liposomes (PEG-DTX-L) cleared rapidly from blood

ABBREVIATIONS: ABC, accelerated blood clearance; AUC, area under the concentration-time curve; CAR, constitutive androstane receptor; DAPI, 4′, 6-diamidino-2-phenylindole; DEX, dexamethasone; DTX, docetaxel; KTZ, ketoconazole; P450, cytochrome P450; PBS, phosphate-buffered saline; PEG, polyethylene glycol; PEG-B-L, blank PEGylated liposomes; PEG$_{2000}$-DSPE, distearoyl phosphoethanolamine-PEG$_{2000}$; PEG-DTX-L, PEGylated liposomal docetaxel; PXR, pregnane X receptor; RT-qPCR, reverse transcription–quantitative polymerase chain reaction; RXRα, retinoid X receptor alpha.

upon repeated injection to the same rat with a time interval of 1–7 days. The strongest magnitude of this phenomenon occurred with a 3-day interval and the phenomenon attenuated with extended time intervals (Wang et al., 2019). We further found the increased activities and expression of cytochrome P450s (P450s), especially CYP3A1 (which metabolizes DTX into the same products as human CYP3A4), may be involved in the accelerated blood clearance (ABC) phenomenon (Vaclavikova et al., 2004). Nevertheless, the detailed mechanism for the induction of P450 activities in the ABC phenomenon is ambiguous. Despite multiple possible mechanisms for inducing P450 activities and expression, the major way is via activation of nuclear receptors, a superfamily of ligand-activated transcription factors. Among these receptors, pregnane X receptor (PXR) and the constitutive androstane receptor (CAR) have been identified as principal regulators with overlapping functions in the transcription of P450 genes involved in oxidative metabolism and elimination of xenobiotics/drugs (Moore et al., 2000; Sinz, 2013; Kanno et al., 2016; Buchman et al., 2018). It has been documented that both PXR and CAR are abundantly expressed in liver, and to a lower level in the kidney and intestine (Willson and Kliewer, 2002). Structurally, PXR and CAR belong to the "orphan receptors" (subfamily NR1) and share approx. 40% amino acid identity in their ligand-binding domains (LBDs) (Xu et al., 2005). In general, PXR and CAR are largely located in the cytoplasmic compartment of hepatocytes and act as transcriptional suppressors by binding with corepressors (Nagy et al., 1997). In the presence of agonist or ligand, a conformational change in the activation of the LBD region is essential for initiating the dissociation of corepressors and favoring recruitment of coactivators. Subsequently, retinoid X receptor alpha (RXRα) as a dimerization partner binds to PXR or CAR, forming a transcriptionally active heterodimer, leading to nuclear translocation, and ultimately resulting in the transcription of target genes upon binding to their response elements in the promoter regions (Mangelsdorf and Evans, 1995; Hashimoto and Miyachi, 2005). It is worth mentioning that many ligands can simultaneously activate PXR and CAR; hence, they regulate the inductive expression of a group of overlapping target genes, including CYP3A4 (homologous to rat CYP3A1), CYP2C9 (homologous to rat CYP2C6), and CYP1A2, which are also most highly expressed in liver (Lehmann et al., 1998; Moore et al., 2000; Wolf et al., 2005; Guengerich, 2008; Tojima et al., 2012; Burkina et al., 2017). Accordingly, from a clinical point of view, activation of PXR and CAR will result in changes in pharmacokinetics for the substrates of these hepatic enzymes, leading to an increased elimination rate of these substrates.

This study was undertaken to ascertain the molecular mechanism of the induction of rat PXR- and/or CAR-P450s axis and their effect on the ABC phenomenon upon repeated injection of PEG-L. We are currently determining the pharmacokinetic parameters of PEG-DTX-L to evaluate the magnitude of the ABC phenomenon. Our previous studies have shown that the induction process of the ABC phenomenon is partly a result of the induced activities and expression of hepatic P450s. Here we unraveled whether nuclear translocation of PXR and CAR occurred in the induction phase of the ABC phenomenon. In that context, therefore, we first detected the expression and localization of PXR and CAR in the hepatocyte nucleus and cytoplasm. Moreover, dexamethasone (DEX), a prototypical inducer of rat PXR through transactivation without effect on CAR (Moore et al., 2000; Shi et al., 2010), was used to characterize the effect of PXR-mediated induction of the CYP3A1-signaling axis in rats. We assessed the impact of DEX on the pharmacokinetic profile of the subsequent injection of PEG-DTX-L. In addition, the gene and protein expression of hepatic PXR and

P450s, as well as alteration of expression and localization of PXR protein in nucleus and cytoplasm, were measured. These data may help to extend our insights into the role of P450s, which are regulated by liver-enriched PXR and CAR, in the induction of the ABC phenomenon.

Materials and Methods

Materials. High purity (>99.0%) DTX and paclitaxel (internal standard), cholesteryl hemisuccinate, and purified hydrogenated yolk lecithin (HEPC) were supplied by Ponsure Biotechnology Co., Ltd. (Shanghai, China). Cholesterol (Chol) was supplied by Sinopharm Chemical Reagent Co., Ltd. (Shanghai, China). 1, 2-distearoyl-sn-glycero-3-phosphoethanolamine-*N*-[methoxy(polyethylene glycol)-2000] (PEG$_{2000}$-DSPE) was obtained from Shanghai Advanced Vehicle Technology Pharmaceutical Ltd. (Shanghai, China). All lipids were used without further purification. A liquid chromatography–mass spectrometry grade of methanol was purchased from Merck (Darmstadt, Germany) and the same of ammonium formate and formic acid from Fluka Analytical (St. Louis, MO). DEX (purity >99.0%) and corn oil were purchased from Yuanye Biotechnology Co., Ltd. (Shanghai, China). For detecting mRNA, SYBR Green PCR Kit (QIAGEN, Frankfurt, Germany), the forward and reverse primers of all target genes (Sangon Biotech Co., Ltd., Shanghai, China), TRIzol reagent (Life Technologies Inc., Carlsbad), and Kit of RevertAid First Strand cDNA Synthesis (Thermo Fisher Scientific, Vilnius, Lithuania) were used. For measuring protein, mouse or rabbit antibodies of anti-CYP2C6, anti-CYP3A1, anti-CYP1A2, anti-CAR, and anti-GAPDH (Abcam, Cambridge, UK), anti-PXR (Abnova, Taipei, Taiwan), anti-RXRα (Proteintech Group, Chicago), anti-Histone H3 (abbkine, CA) (ZSJQ Biotechnology Co., Ltd., Beijing, China), and enhanced chemiluminescence (ECL) reagent kit (Thermo Fisher Scientific, Rockford) were used. The HRP-conjugated goat anti-rabbit or mouse IgG (H+L), fluorescein (FITC)-conjugated goat anti-rabbit IgG (H+L), and rhodamine (TRITC)-conjugated goat anti-mouse IgG (H+L) were purchased from BioSharp life sciences (Hefei, China). 4′, 6-diamidino-2-phenylindole (DAPI) and antifade mountant, RIPA lysis buffer, and BCA protein assay kit were obtained from Beyotime Biotechnology (Shanghai, China). Nuclear and cytoplasmic extraction kit was purchased from BestBio (Shanghai, China). Ultrapure water was provided by means of a Milli-Q Reference Ultrapure Water apparatus (Merck). Other chemicals were analytical grade commercially available.

Preparation of PEGylated Liposomes. Using a single-factor analysis and orthogonal test, our previous studies described the optimal formulation of PEG-DTX-L. The solvent injection method was used to prepare PEG-DTX-L (Wang et al., 2019). Briefly, the lipid phase including PEG$_{2000}$-DSPE, purified HEPC, Chol, and Chol hemisuccinate were dissolved in moderate amounts of absolute ethanol and heated up to 50°C to obtain a homogeneous solution. Following the addition of DTX, the hot mixtures were then immediately injected into phosphate-buffered saline (PBS; pH 7.4), maintained at the same temperature with a stirring of 800 rpm for 2 hours to form PEG-L. Subsequently, the harvested multilamellar liposomes were passed through homogenization at 10,000 rpm for 15 minutes, and small unilamellar PEG-DTX-L was obtained. The physicochemical characteristics of PEG-DTX-L, including morphology, particle diameter, polydispersity index (PDI), zeta potential, differential scanning calorimetry, and in vitro release kinetics were determined, and the entrapment efficiency (EE) was calculated indirectly by validated high-performance liquid chromatography (Waters 1525; Waters) analysis. The transmission electron micrograph of PEG-DTX-L showed a spherical shape with nearly monodisperse size distribution in the nanometer scale. The values of mean particle size, PDI, zeta potential, and EE (%) for PEG-DTX-L were 118.13 ± 2.25 nm, 0.173 ± 0.02, −32.40 ± 1.04 mV, and (96.62 ± 0.95)%, respectively. The well sustained DTX release from the liposomes could be attributed to the incorporation of DTX into the hydrophobic space of the phospholipid bilayer. Taken together, the optimal formulation is considered suitable for PEG-DTX-L preparation because of its high EE and well characterized size distribution, in addition to its stable structure and perfectly controlled release profile. The same procedure as for PEG-DTX-L without adding DTX was performed to prepare blank PEGylated liposomes (PEG-B-L). As expected, physicochemical characteristics of PEG-B-L was quite comparable with PEG-DTX-L.

TABLE 1

Injection protocols for PEGylated liposomes and DEX

Control (0 day) indicates the group received only a single dose of PEG-DTX-L (containing 0.05 μmol of PEG-DSPE/kg). 3 Day indicates the animals received repeated injections of PEG-L with a 3-day interval. DEX+PEG-L represents i.p. 100 mg/kg dexamethasone once daily for three consecutive days following a single injection of 2.5 mg/kg PEG-DTX-L.

Group	First Injection	Time Interval (days)	Second Injection (i.v. 2.5 mg/kg)
Control (0 day)	—	0	PEG-DTX-L
3 Day	PEG-B-L (i.v. 0.05 μmol/kg)	3	PEG-DTX-L
DEX+PEG-L	DEX (i.p.100 mg/kg) for 3 consecutive days	3	PEG-DTX-L

i.p., intraperitoneal injection; i.v., tail intravenous injection; PEG-L, PEGylated liposomes.

Ethics Statement for Animals. Sprague-Dawley rats (5- to 6-weeks old, male, 220 ± 15 g) were provided by the Experimental Animal Center of Anhui Medical University (Hefei, China). Rats were housed in conditions of 23–27°C, 55%–65% humidity, and a 12-hour light-dark cycle for 7 days and then randomly divided into different groups. Standard food and water were fed to rats ad libitum. All procedures were performed in the light of animal care principles evaluated and approved by Institutional Animal Care and Use Committee, Anhui University of Chinese Medicine.

Liver Tissues of Different Time Intervals between Two Injections. Our previous studies revealed that the time interval between two injections of PEG-L has significant influence on the magnitude of the ABC phenomenon, owing to the different activities and expressions of CYP3A1, CYP2C6, and CYP1A2 in various time intervals (Wang et al., 2019). To evaluate whether the upstream transcription factors affect the expression of these hepatic P450 genes in different test groups (1 day, 3 days, 5 days, and 7 days), rats were intravenously injected (tail vein) with two doses of PEG-L at four different time intervals, PEG-B-L (containing 0.05 μmol of PEG-DSPE/kg) on 0 day and then 2.5 mg/kg PEG-DTX-L after 1, 3, 5, or 7 days. Rats in group 0 day received only a single injection of 2.50 mg/kg of PEG-DTX-L. A single dose of an equal volume of PBS was injected into rats and was regarded as the normal control. Each group had six rats. After the last administration at 12 hours, liver tissues were collected under isoflurane anesthesia and stored in a liquid nitrogen container until measurement.

Pharmacokinetic and Biodistribution of PEGylated Liposomes. To investigate whether PXR and P450s genes are involved in the ABC phenomenon, the effectively specific PXR inducer (DEX) was employed in this study. The dose and method of administration of DEX was referenced in a previous report (De Martin et al., 2014). The induction study consisted of three groups ($n = 6$ for each group). Treatment was as follows: To induce PXR, rats in group 1 were pretreated with an i.p. dose (100 mg/kg, dissolved in 3 ml corn oil) of DEX once daily for 3 days consecutively followed on the last day by a single injection of 2.5 mg/kg of PEG-DTX-L (containing 0.05 μmol of PEG$_{2000}$-DSPE/kg, called the DEX+ PEG-L group); rats in group 2 were treated with the first injection of 0.05 μmol/kg PEG-B-L on the 1st day and the injection of 2.5 mg/kg of PEG-DTX-L was repeated on the 4th day (called group 3 day); rats in group 3 were treated with only a single injection of 0.05 μmol of PEG-DTX-L and acted as a control group (called group 0 day). It must be noted that the molality of PEG-L represents the content of PEG$_{2000}$-DSPE, not drug. The detailed dosing schedule for PEG-L and DEX are displayed in Table 1.

Sample preparation (blood, liver, and spleen) and the detection method for DTX levels in these samples are the same as our previous studies (Wang et al., 2019). Paclitaxel was used as internal standard. DTX in plasma and tissue samples was quantified by high-pressure liquid chromatography–tandem mass spectrometry (Supplemental Methods). The method has been validated in our previous studies according to the FDA guideline for bioanalytical method validation (Wang et al., 2019). A noncompartmental model was applied to calculate the pharmacokinetic parameters in DAS 2.0 software (Shanghai Bojia Medical Technology co., Ltd, Shanghai, China).

Determination of Total mRNA and Protein Expression in Liver Samples. The quantification analysis for evaluating total mRNA and protein in liver samples was performed with reverse transcription–quantitative polymerase chain reaction (RT-qPCR) and Western blotting, respectively. The detailed procedures (Supplemental Methods and Supplemental Table S1) were followed as described before (Wang et al., 2019).

Subcellular Fractionation. For the evaluation of nucleus localization of hepatocyte PXR, CAR, and RXRα protein, a commercial nuclear and cytoplasmic extraction kit was used to fractionate nuclear and cytoplasmic protein according to the protocol recommended by the manufacturer. The quantitative changes in these target proteins from nucleus or cytoplasm were measured by Western blotting as mentioned above. GAPDH and histone H3, respectively, were employed as the loading controls for the cytoplasmic and nuclear target proteins.

Immunofluorescence Staining. After fixation with 4% paraformaldehyde at 4°C for 24 hours, liver tissues were dehydrated in 30% sucrose at 4°C for 8 hours, and then 8-μm-thick sections were obtained with a freezing microtome (Leica CM1900; Leica Microsystems, Germany). After blockade with 10% normal goat serum (containing 0.4% Triton X-100), the sections were incubated overnight with primary or anti-RXRα or anti-CAR antibody (1:1000) at 4°C. Subsequently, the sections were labeled with a 1:200 concentration of fluorescein-conjugated goat anti-rabbit IgG (H+L) or rhodamine (TRITC)-conjugated goat anti-mouse IgG (H+L) for 2 hours at room temperature. Finally, DAPI (1 μg/ml) was used for staining the nuclei for 10 minutes. After a washing, the sections were mounted with antifade mountant on adhesion microscope slides. The images captured with an Olympus FV1000 confocal microscope (Olympus Corp., Tokyo, Japan) at 40×.

Statistics. All data are presented as mean ± S.D. of at least three independent experiments. Statistical analyses were performed by SPSS 23.0 software (IBM Corp., Armonk, NY). Significant differences were analyzed according to one-way analysis of variance followed by a Student-Newman-Keuls post-hoc test. Comparison of the differences in pharmacokinetic parameters within each group was performed by nonparametric test (Kruskal-Wallis) followed by Dunn's test. A P value of less than 0.05 was considered statistically significant.

Results

The Expression of Hepatic PXR and CAR Induced by Repeated Injection of PEG-L

Determination of the mRNA and Total Protein Expression of Hepatic PXR and CAR. Despite the fact that increased expression of CYPs 3A1, 2C6, and 1A2 (especially for CYP3A1) has been proven to be involved in the ABC phenomenon (Wang et al., 2019), we wondered if these P450 genes, in the induction of the ABC phenomenon, are regulated by upstream transcription regulators such as PXR and CAR. For this purpose, we first detected the mRNA and total protein expression of these two nuclear receptors in liver upon repeated injection of PEG-L with four different time intervals (1, 3, 5, and 7 days) in rats (groups 1 day, 3 day, 5 day and 7 day). Rats in group 0 day were only treated with a single dose of PEG-DTX-L. Additionally, rats receiving a single injection of an equal volume of PBS were used as the normal control. In comparison with group 0 day, a significant fold increase in PXR mRNA with approx. double increase of PXR protein expression was observed in groups 3 day and 5 day, and approx. 1.3-fold of increase in PXR protein expression was observed in group 7 day; Concerning CAR expression, increased CAR mRNA was detected in groups 3 day, 5 day, and 7 day with increased CAR protein expression in groups 3 day and 5 day (Fig. 1). It should be noted that the mRNA and protein expression of PXR in
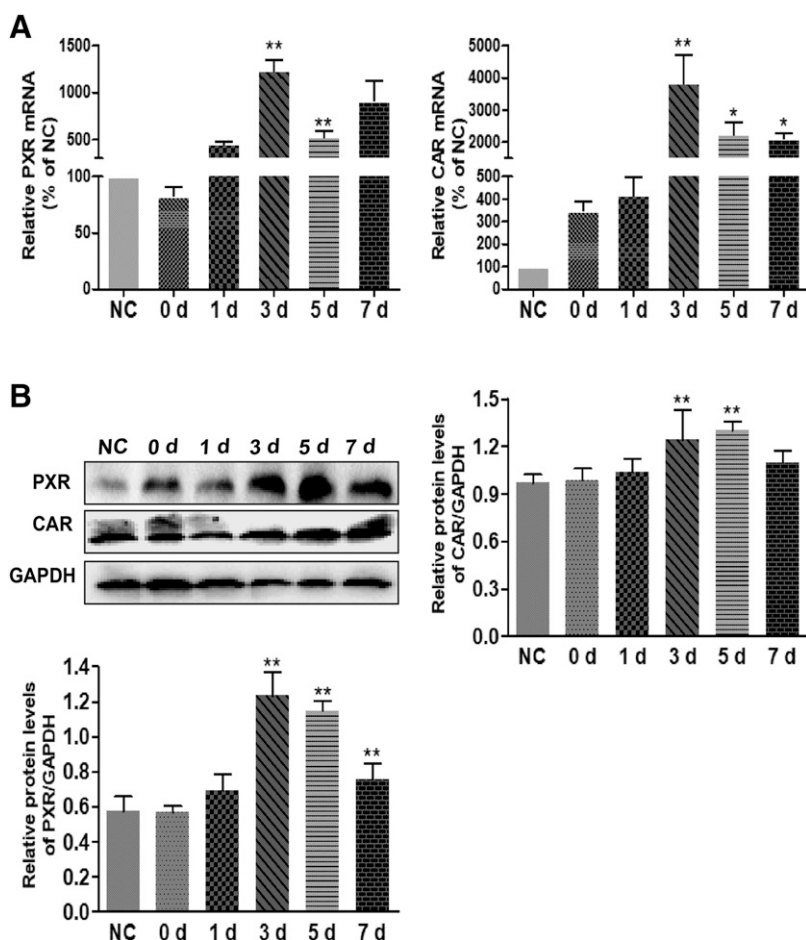
Fig. 1. Effect of repeated injection of PEG-L on the mRNA and total protein expression of PXR and CAR in rat liver. The hepatic PXR and CAR expression profiles were determined after the first injection of PEG-L followed by a subsequent injection of PEG-DTX-L with different time intervals, including 1, 3, 5, and 7 days (1 day, 3 day, 5 day, and 7 day). 0 day indicates the group only received a single injection of PEG-DTX-L. Normal control group was injected with a single injection of equal volume PBS. The liver samples were obtained as described in the *Materials and Methods* section. (A) RT-qPCR analysis of the relative mRNA transcript levels of hepatic PXR and CAR. Using β-actin as an endogenous reference gene, the values were normalized to the control group and fold change was calculated by $2^{-\Delta\Delta CT}$ method. (B) The relative protein level of hepatic PXR and CAR were analyzed by Western blotting. Bar graphs show quantitative evaluation of PXR and CAR bands by densitometry from triplicate independent experiments. Each band density was evaluated by ImageJ software and these data were calculated as percentages compared with GAPDH (a housekeeping protein). Data are presented as the mean $\pm$ S.D. ($n = 5$ to 6). *$P < 0.05$; **$P < 0.01$ compared with the 0 day group. PEG-L, PEGylated liposomes.

group 3 day were highest among the four test groups, and then slowly decreased with longer time intervals, which is consistent with the reduced trends of the P450s expression and the magnitude of the ABC phenomenon mentioned in our previous studies (Wang et al., 2019).

Determination of the Nuclear and Cytoplasmic Protein Expression of Hepatic PXR, RXRα and CAR. Since nuclear translocation and the formation of protein heterodimer with RXRα are required for PXR and CAR to initiate the transcription of target genes, the issue of whether repeated injection of PEG-L induced nuclear translocation and heterodimerization of hepatic PXR, CAR, and RXRα were investigated by Western blotting and immunofluorescence colocalization analysis, respectively. As for PXR, a dramatically increased protein expression was found in the hepatocyte cytoplasm and nuclear fractions in groups 3 day, 5 day, and 7 day compared with 0 day group. Concerning RXRα expression, a significantly decreased cytoplasmic RXRα protein was detected in 3 day, 5 day, and 7 day groups accompanied by obviously increased nuclear protein in groups 3 day and 5 day compared with the 0 day group. The reason for this difference between the cytoplasmic and nuclear RXRα protein may be attributable in part to nuclear translocation by formation of heterodimer with PXR. Unlike the former receptors, CAR protein was found to be increased only in the cytoplasm of groups 3 day, 5 day, and 7 day compared with the 0 day level, and no significant change in nuclear levels were found among these groups (Fig. 2).

Consistently, double immunofluorescent staining revealed that PXR protein colocalized with RXRα protein (PXR-RXRα) in the hepatocyte nucleus (Fig. 3). In comparison with 0 day group, the most apparent

nuclear colocalization of PXR-RXRα was observed in hepatocytes of groups 3 day and 5 day and was attenuated in group 7 day. As expected, we failed to detect significant nuclear translocation for CAR protein in the four test groups (Supplemental Fig. S1). Taken together, these data provide strong evidence that repeated injection leads to the colocalization of PXR and RXRα in cell nuclei, which is probably responsible for the upregulation of P450s transcription and/or protein expression.

Effects of Pretreatment of PXR Inducer on the Pharmacokinetics of the Subsequent Dose of PEG-DTX-L

To clarify the potential of PXR in inducing P450s production in the ABC phenomenon, DEX was employed as a PXR effective inducer. By pretreating with DEX or PEG-L before an injection of PEG-DTX-L with a 3-day interval, the effects of DEX and PEG-L on the pharmacokinetic profile of the subsequent dose of PEG-DTX-L in rats are shown in Fig. 4A and Table 2. Pharmacokinetic analysis revealed that a significantly decreased area under the plasma concentration–time curve from 0 to the last quantifiable time point (AUC_{0-t}) and half-life ($t_{1/2}$), as well as increased plasma clearance, were observed both in the repeated injection of PEG-L group (group 3 day) and group DEX+PEG-L compared with control (0 day), suggesting that an accelerated clearance of the subsequent dose of PEG-DTX-L from blood circulation occurred both in group 3 day and group DEX+PEG-L. A concomitant reduction in accumulation of DTX in liver was also observed, together with an increased level of DTX in spleen as shown in group DEX+PEG-L (Fig. 4B), which might be attributable to the activation of PXR involved in the induction of hepatic CYP3A1 gene transcription. The $AUC_{C/T}$ (ratio of AUC of the
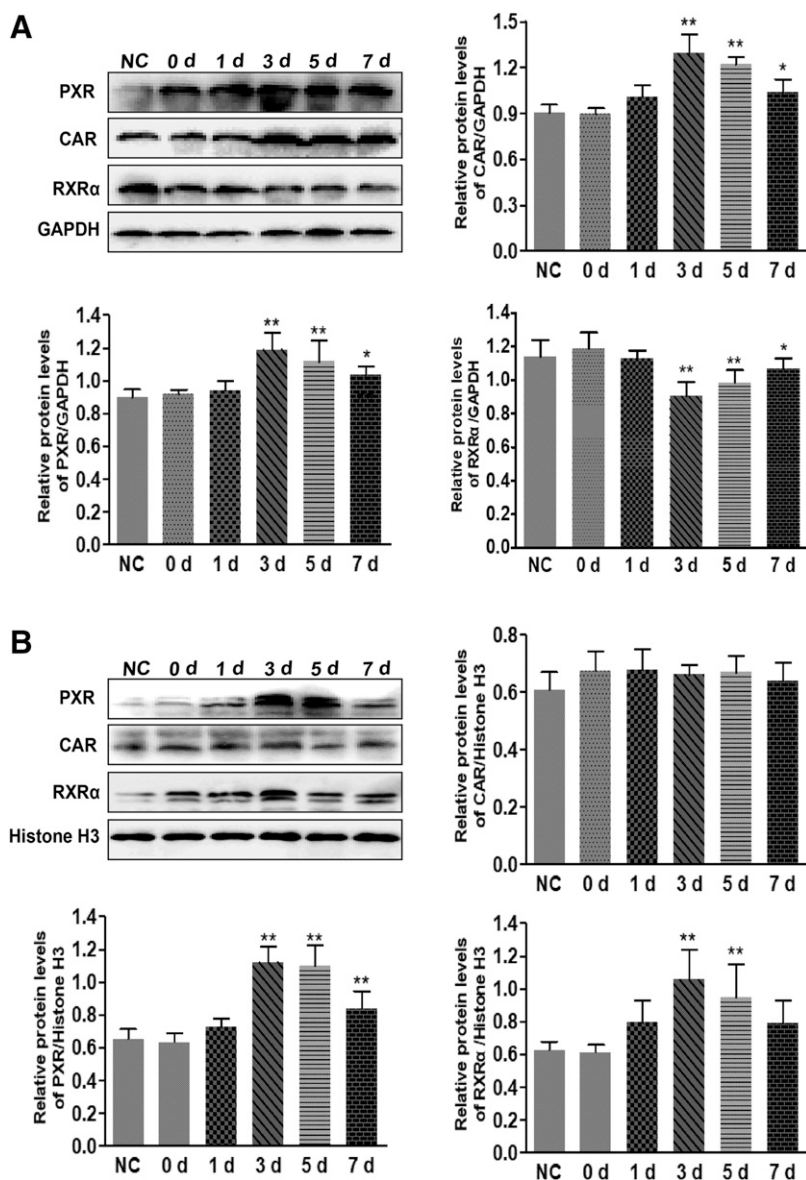
Fig. 2. Effect of repeated injection of PEG-L on the nuclear and cytoplasmic protein expression of hepatic PXR, RXRα, and CAR in rats. (A) The relative cytoplasmic protein expression of hepatic PXR, RXRα, and CAR were analyzed by Western blotting. Bar graphs show quantitative evaluation of PXR, RXRα, and CAR bands by densitometry from three separate experiments. (B) The relative nuclear protein expression of hepatic PXR, RXRα, and CAR were analyzed by Western blotting. Bar graphs show quantitative evaluation of PXR, RXRα, and CAR bands by densitometry from three separate experiments. Each band density was evaluated by ImageJ software and these data were calculated as percentages compared with GAPDH or histone H3. Data are presented as the mean ± S.D. (n = 5 to 6). *P < 0.05; **P < 0.01 compared with the 0 day group. PEG-L, PEGylated liposomes.

control group to the test group) and $t_{1/2\text{-}C/T}$ (ratio of $t_{1/2}$ of the control group to the test group) were previously considered as key markers to evaluate the altered pharmacokinetics of these experimental groups. Thereby the ABC phenomenon was assessed by measuring AUC and $t_{1/2}$ of the experimental payload (DTX) (Xu et al., 2015). Notably, the pharmacokinetic profile and the magnitude of the ABC phenomenon of group DEX+PEG-L are comparable with group 3 day (Table 3). These results clearly indicate that the activation of PXR induced by repeated injection of PEG-L at least partially facilitates the rapid elimination of the subsequent dose of PEG-DTX-L in rats.

Effects of the Pretreatment of PXR Inducer on the Expression of Hepatic PXR, CAR, and P450s

Determination of the mRNA and Total Protein Expression of PXR, CAR, and P450s in Liver. In comparison with the control group, intraperitoneal preinjection with DEX for three consecutive days combined with a subsequent injection of PEG-DTX-L (group DEX+PEG-L) increased mRNA and total protein expression of PXR and its target genes, including CYP3A1, CYP2C6, and CYP1A2 in

liver, which is comparable with those of group 3 day. As expected, no significant difference was observed for the mRNA and total protein expression of CAR between the DEX+PEG-L and control groups, suggesting DEX selectively induces PXR (Supplemental Fig. S2).

Determination of the Nuclear and Cytoplasmic Protein Expression of Hepatic PXR and RXRα. The results for nuclear translocation of group DEX+PEG-L and group 3 day are showed in Fig. 5. Compared with group 0 day, the relative intensity of the immunereactive band of PXR protein was significantly increased both in the hepatocyte cytoplasm and nucleus in group DEX+PEG-L, and a similar result was present in group 3 day. Meanwhile, RXRα protein level was found to be significantly downregulated in cytoplasm and upregulated in nucleus in both test groups, which may be attributed partly to the nuclear translocation by formation of a heterodimer with PXR. In addition, no significant difference in nuclear translocation of CAR protein was detected, which suggests a selective inductive effect of DEX on the activation of PXR.

To more deeply explore the colocalization of hepatocyte PXR and RXRα proteins, double immunofluorescent staining analysis was
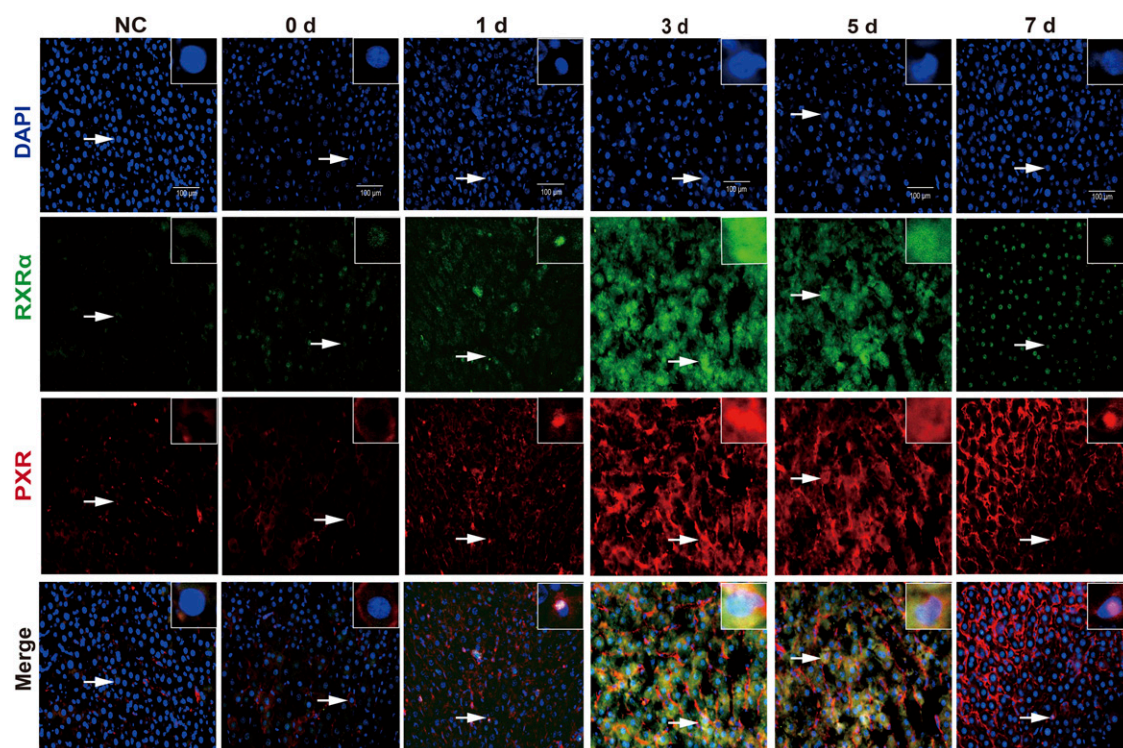
Fig. 3. Double immunofluorescence staining showed the nuclear translocation of hepatic PXR and RXRα proteins in the hepatocyte nucleus ($n = 3$). PXR and RXRα are shown in red and green, respectively, and the nuclei were stained with DAPI (blue). Zero day indicates the group only received a single dose of PEG-DTX-L. One day, 3 day, 5 day, and 7 day indicate rats received repeated injection of PEG-L with different time intervals (1, 3, 5, and 7 days, respectively). Normal control group (NC) was injected with a single injection of equal volume PBS. Scale bar, 100 μm.

performed in the following groups. Control rats received repeated injection of PEG-L with a 3-day interval; group "3 day (KTZ+)" indicates the samples obtained from our previous studies in which rats were pretreated with oral administration of 100 mg/kg per day of KTZ (ketoconazole, a strong inhibitor of CYP3A1 in rats) for seven consecutive days, coadministered with repeated injection of PEG-L with a 3-day interval; the detailed dosing protocol for group DEX+PEG-L is given in Table 1. As demonstrated in Supplemental Fig. S3, no obvious nuclear translocation and colocalization of PXR and RXRα proteins occurred in the group 3 day (KTZ+) compared with control level, whereas a strong colocalization of PXR and RXRα proteins was recovered in group DEX+PEG-L. Taken together, these data imply that pretreatment with P450s inhibitor leads to the inhibition of nuclear translocation and colocalization of PXR and RXRα proteins upon repeated injection of PEG-L. In contrast, PXR inducer enhanced nuclear translocation and colocalization of PXR and RXRα proteins, suggesting that the activation of PXR in response to sequential injections of PEG-L induces the increased P450s production, which may be partly responsible for the rapid clearance of the second dose of PEG-L.

Discussion

P450s implicated in drug metabolism and elimination are induced by drug/xenobiotic-activated nuclear receptors, which are ligand-activated transcription factors. Our previous studies have shown the induction of P450s (such as CYP3A1, CYP2C6, and CYP1A2) is largely responsible for the repeated injection of PEG-L–induced ABC phenomenon (Wang et al., 2019). Both in human and rat, PXR and CAR are recognized as primary transcription factors that activate hepatic genes encoding these P450 isoforms (Lehmann et al., 1998; Moore et al., 2000; Guengerich,

2008; Burkina et al., 2017). A close link has been identified between these nuclear receptors and diverse diseases, including metabolic diseases, liver diseases, and so on, which can be treated by established therapeutic PXR and/or CAR agonists on the market (Shah et al., 2007; Gao and Xie, 2012; Rysä et al., 2013). Consequently, understanding the signaling network of PXR- and/or CAR-target genes and their contributions in the development of certain diseases will facilitate the discovery of agents that target the related pathways for relevant therapeutic applications (Banerjee et al., 2015). To date, few attempts have been made at unraveling the association between nuclear receptors-P450s axis and the ABC phenomenon owing to neglect of the role of P450s in the ABC phenomenon. We recently reported the contribution of P450s in the ABC phenomenon (Wang et al., 2019). It seemed therefore particularly interesting to investigate whether the activation of PXR and or CAR and their target genes (P450s) are involved in the ABC phenomenon. The present work aimed to provide more valuable data for studying the effect of PXR/CAR–P450s axis on the induction of ABC phenomenon.

Given the expression of PXR/CAR as well as P450s in the liver of rats (Willson and Kliewer, 2002; Guengerich, 2008), we first examined if repeated injection of PEG-L (with different time intervals) induced the nuclear translocation of hepatic PXR/CAR in rats. In this study, PXR protein was found to be markedly upregulated both in liver cell cytoplasm and nucleus in the repeated injection groups compared with control, resulting in a significant increase of total PXR protein (Figs. 1 and 2). Unlike PXR, upregulation of hepatic CAR protein upon repeated injection of PEG-L was the result of increased CAR protein in the hepatocyte cytoplasm, and no significant increase in nuclear CAR was observed, indicating a lack of nuclear translocation of CAR (Fig. 2; Supplemental Fig. S1). These results are in agreement
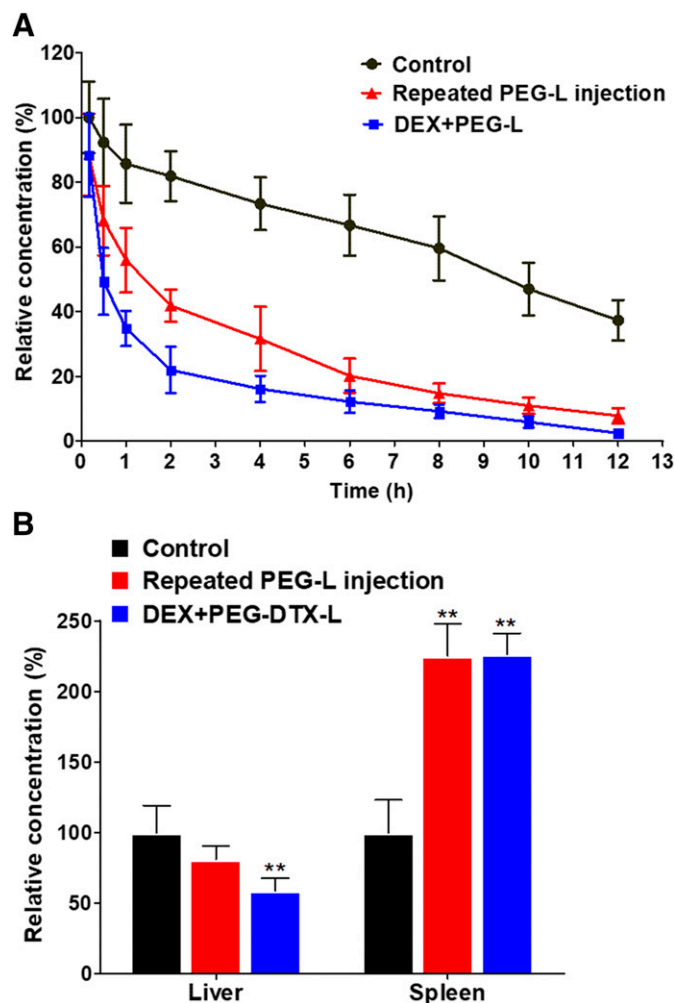
Fig. 4. Effect of the pretreatment of PXR inducer on the pharmacokinetics of the subsequent dose of PEG-DTX-L. (A) The mean concentration-time (0–12 hours) profile of DTX in rats after a second injection of PEG-DTX-L. The relative concentration represents the relative ratio with the initial concentration (at 10 minutes) of control. (B) Liver and spleen distribution (12 hours) of DTX in rats after a second injection of PEG-DTX-L. The relative concentration represents the relative ratio with the liver and spleen concentration of control, respectively. $**P < 0.01$ compared with 0 day ($n = 6$, mean $\pm$ S.D.).

with the findings of Moore et al. (2000), which emphasized that DEX specifically activated PXR but not CAR in rodents. Generally, PXR heterodimerizes with RXRα to form a transcriptionally active complex (PXR-RXRα heterodimer) and translocates to the hepatocyte nucleus

to activate target gene transcription (Kawana et al., 2003; Squires et al., 2004). As mentioned above, the decreased RXRα protein in hepatocyte cytoplasm and increased RXRα protein in hepatocyte nucleus were significantly different between the control group and the test groups especially for groups 3 day and 5 day. Consistent with this, immunofluorescent colocalization staining analysis arrived at similar results, that is, a strong colocalization of PXR and RXRα proteins in the hepatocyte nucleus was observed in the test groups, but not in the control group (Fig. 3). These results are in line with our previous study, which demonstrated increased expression of P450s, including CYP3A1, CYP2C6, and CYP1A2 (Wang et al., 2019). These findings, although preliminary, suggest that the repeated injection of PEG-L leads to the nuclear translocation of PXR and subsequent transcription of the inducible P450 genes.

It is worth mentioning the fact that DTX is predominantly metabolized to the same metabolites by CYP3A in human (CYP3A4/5) and rats (CYP3A1/2) (Vaclavikova et al., 2004). PXR has been recognized as a crucial regulator of CYP3A4 by binding to a response element in the CYP3A4 promoter (Lehmann et al., 1998; Kliewer et al., 2002). In general, a broad spectrum of ligands belonging to drugs or endogenous compounds can induce PXR, leading to the activation of the downstream target genes involved in their metabolism and subsequently contributing to their rapid clearance (di Masi et al., 2009; Smutny et al., 2013). We therefore hypothesized that the activation and nuclear localization of PXR is induced upon repeated injection of PEG-L, resulting in a significant increase in CYP3A1, which is then implicated in the accelerated clearance of DTX from the liposomes in blood circulation and liver.

DEX, a typical rat PXR agonist for inducing the expression of CYP3A, is usually regarded as a tool compound to induce CYP3A activity (Kliewer et al., 1998; Lehmann et al., 1998). To better clarify the mechanism of PXR-P450s axis and its role in the ABC phenomenon, we assessed the effects of DEX on the pharmacokinetics of PEG-DTX-L and the expression of its target P450 genes compared with those of repeated injection of PEG-L. The pharmacokinetic study demonstrated that intraperitoneal preinjection of DEX contributed to an ABC phenomenon similar to that observed with repeated injection of PEG-L (Fig. 4A). Meanwhile, upregulated expression of P450s (especially CYP3A1) mRNA and protein was found both in group 3 day and group DEX+PEG-L compared with control (group 0 day) level, which may be attributable to the activation of PXR and the nuclear translocation of PXR-RXRα. The rodent CAR was unable to respond to DEX (Fig. 5), which indicates that DEX is specific for activating PXR. On the basis of DTX pharmacokinetics, repeated PEG-L injections behaved in a manner very similar to DEX pretreatment. However, the PEG-L results are

TABLE 2

Pharmacokinetic parameters of PEG-DTX-L after intravenous injection in rats (mean $\pm$ S.D., $n = 6$)

Control (0 day) indicates the group received only a single injection of PEG-DTX-L. 3 Day indicates the animals received repeated injections of PEG-L with a 3-day interval. DEX+PEG-L represents i.p. 100 mg/kg dexamethasone once daily for 3 consecutive days following a single injection of 2.5 mg/kg PEG-DTX-L.

Parameter	Control (0 day)	Repeated Injection Group	
		3 Day	DEX+PEG-L
AUC$_{(0-t)}$ (μg/l·h)	7797.01 $\pm$ 1844.54	3124.39 $\pm$ 477.38*	1763.52 $\pm$ 322.25**
MRT$_{(0-t)}$ (h)	5.13 $\pm$ 0.26	3.89 $\pm$ 0.26**	3.79 $\pm$ 0.27*
t$_{1/2}$ (h)	6.47 $\pm$ 1.27	4.21 $\pm$ 1.27*	3.55 $\pm$ 0.96*
CLz (l/h per kilogram)	0.24 $\pm$ 0.07	0.71 $\pm$ 0.12	1.32 $\pm$ 0.27**

AUC$_{0-t}$, area under the plasma concentration-time curve from time 0 to the last quantifiable time point; CLz, plasma clearance; MRT$_{0-t}$, mean residence time from time 0 to the last quantifiable time point; t$_{1/2}$, half-life.
$*P < 0.05$; $**P < 0.01$ compared with control (0 day).

TABLE 3

Pharmacokinetic parameter ratios for the magnitude of ABC phenomenon (mean ± S.D., $n = 6$)

Group control (0 day) and DEX+ PEG-L as mentioned in Table 2.

Parameter	Control (0 day)	3 Day	DEX+ PEG-L
$^{\triangle}AUC_{C/T}$	1.00	2.50 ± 0.22	4.42 ± 0.78
$^{\triangle}t_{1/2-C/T}$	1.00	1.54 ± 0.24	1.82 ± 0.17

AUC_{0-t}, area under curve from time 0 to t; d, day; $t_{1/2}$, half-life. $^{\triangle}$Represents a pharmacokinetic parameter ratio of the control group to the test group.

not crisply in line with DEX results, as DEX did not cause CAR expression changes, whereas PEG-L resulted in increased CAR expression in the cytoplasm. These differences need to be noted, as it would be possible that DEX induces P450 expression solely via PXR and yet PEG-L could induce via a joint PXR/CAR mechanism. However, when coupled with the increases in PXR and RXR concentrations in the nucleus induced by repeated injection of PEG-L, the data strongly suggest a primary involvement of PXR activation in the induction of P450s in the ABC phenomenon.

Additionally, previous studies have established that KTZ can competitively inhibit the activity and expression of CYP3A1 through PXR-regulated gene transcription (Huang et al., 2007; Ma et al., 2008). Fluorescence microscopy proved that KTZ pretreatment suppressed the nuclear translocation of PXR-RXRα dimer in hepatocytes, which was recovered by DEX (Supplemental Fig. S3). These data provide new clues for a better understanding of the significance of PXR-P450s signaling pathways in the induction process of the ABC phenomenon.

The veracity of these results is subject to certain limitations. First, species differences result in a lot of intriguing issues regarding specificity. Although most human and rodent nuclear receptor homologous sequences share more than 90% amino acid identity, the human and rodent PXR and CAR respectively share only approx. 76% and 70% sequence homology, which is believed to be responsible for the substantial differences in species-specific PXR and CAR activation and target-genes induction (Moore et al., 2000;

Maglich et al., 2001). For example, rifampicin is a strong inducer of human PXR but has no induction potential for rodent PXR. In contrast, DEX drastically activates rodent PXR but is a weak activator of human PXR. Therefore, multiple humanized/transgenic mouse models for PXR/CAR, PXR/CYP3A4, and PXR/CAR/CYP3A4 may provide more valuable information for assessing specific human drug responses in relation to drug metabolism and pharmacokinetics (Ma et al., 2008; Hasegawa et al., 2011; Scheer et al., 2015). Second, the present findings would be more credible if a specific inhibitor of PXR had been employed. Unfortunately, an appropriate PXR-specific inhibitor has not yet been generated. In addition, no significant nuclear translocation of CAR protein was observed; however, the role of CAR in the ABC phenomenon cannot be totally ruled out. Although drug-induced specific intracellular signal cascades can activate receptor phosphorylation by various kinases, which ultimately result in CAR activation, CAR may not interact with a drug directly (Smutny et al., 2013). Another possibility is that crosstalk by CAR with PXR or transcription factors controlling the networks that positively or negatively regulate the expression of downstream genes indirectly affects xenobiotic/drug disposition (Pascussi et al., 2008; Pavek, 2016). In spite of these limitations to the results, the present research explored for the first time the significance of the PXR-P450s axis on drug metabolism and pharmacokinetics of the repeated injection of PEG-L, a still novel and meaningful result for elucidating the mechanism of the ABC phenomenon and evaluating useful liposomal drug formulations requiring multiple injections. In future work, we will undertake more exploration to validate our present deductions and expand the roles of transcriptional regulators of P450 genes in the ABC phenomenon.

In summary, the evidence from this study suggests that nuclear receptors, especially PXR, are partially responsible for the increased expression of inducible P450 enzymes involved in the ABC phenomenon in rats. The rapid clearance of the second dose from circulation upon repeated injection of PEG-L is similar to the effect of DEX coadministered with an injection of PEG-DTX-L—both result from activation of the PXR-CYP3A1 axis. These data
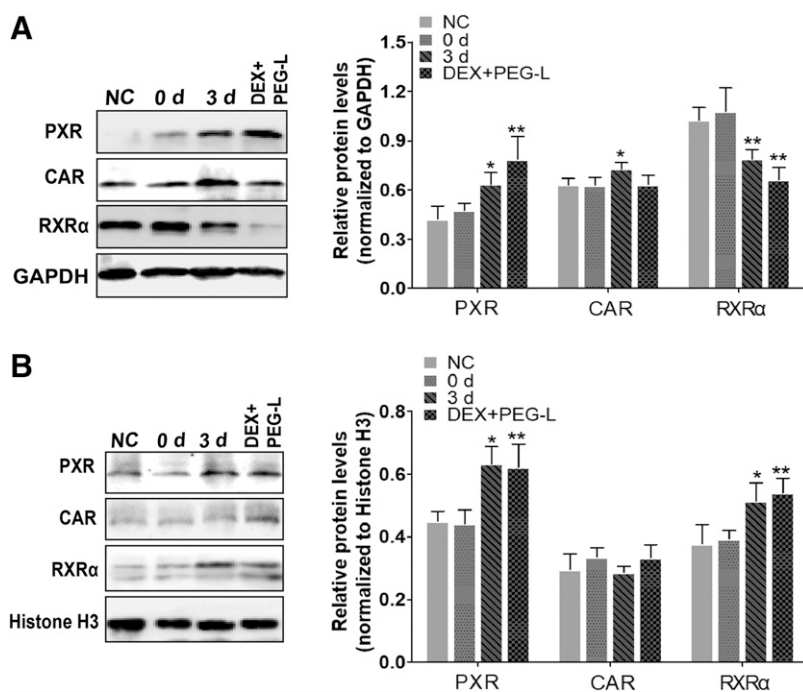

Fig. 5. Effect of the pretreatment of PXR inducer on the location of PXR, CAR, and RXRα in hepatocytes. (A) The relative cytoplasmic protein expression of hepatic PXR, CAR, and RXRα were analyzed by Western blotting. Bar graphs show quantitative evaluation of PXR, CAR, and RXRα bands by densitometry from three independent experiments. (B) The relative nuclear protein expression of hepatic PXR, CAR, and RXRα were analyzed by Western blotting. Bar graphs show quantitative evaluation of PXR, CAR, and RXRα bands by densitometry from triplicate separate experiments. Each band density was evaluated by ImageJ software and these data were calculated as percentage compared with GAPDH or histone H3. Data are presented as the mean ± S.D. ($n = 5$ to 6). *$P < 0.05$; **$P < 0.01$ compared with 0 day group.

highlight the significance of the PXR-P450s axis in the ABC phenomenon and provided new prospects for the therapeutic potential of targeting PXR in clinical practice.

Acknowledgments

Authorship Contributions

Participated in research design: F. Wang, Peng, Chen.

Conducted experiments: F.Wang, H. Wang, Wu, Ye.

Contributed new reagents or analytic tools: L. Wang, Zhang.

Performed data analysis: F. Wang, H. Wang, L. Wang, Zhang.

Wrote or contributed to the writing of the manuscript: F. Wang, H. Wang, Wu.

References

Banerjee M, Robbins D, and Chen T (2015) Targeting xenobiotic receptors PXR and CAR in human diseases. *Drug Discov Today* 20:618–628.

Buchman CD, Chai SC, and Chen T (2018) A current structural perspective on PXR and CAR in drug metabolism. *Expert Opin Drug Metab Toxicol* 14:635–647.

Burkina V, Rasmussen MK, Pilipenko N, and Zamaratskaia G (2017) Comparison of xenobiotic-metabolising human, porcine, rodent, and piscine cytochrome P450. *Toxicology* 375:10–27.

De Martin S, Gabbia D, Albertin G, Sfriso MM, Mescoli C, Albertoni L, Paliuri G, Bova S, and Palatini P (2014) Differential effect of liver cirrhosis on the pregnane X receptor-mediated induction of CYP3A1 and 3A2 in the rat. *Drug Metab Dispos* 42:1617–1626.

di Masi A, De Marinis E, Ascenzi P, and Marino M (2009) Nuclear receptors CAR and PXR: molecular, functional, and biomedical aspects. *Mol Aspects Med* 30:297–343.

Gao J and Xie W (2012) Targeting xenobiotic receptors PXR and CAR for metabolic diseases. *Trends Pharmacol Sci* 33:552–558.

Guengerich FP (2008) Cytochrome p450 and chemical toxicology. *Chem Res Toxicol* 21:70–83.

Hasegawa M, Kapelyukh Y, Tahara H, Seibler J, Rode A, Krueger S, Lee DN, Wolf CR, and Scheer N (2011) Quantitative prediction of human pregnane X receptor and cytochrome P450 3A4 mediated drug-drug interaction in a novel multiple humanized mouse line. *Mol Pharmacol* 80:518–528.

Hashimoto Y and Miyachi H (2005) Nuclear receptor antagonists designed based on the helix-folding inhibition hypothesis. *Bioorg Med Chem* 13:5080–5093.

Huang H, Wang H, Sinz M, Zoeckler M, Staudinger J, Redinbo MR, Teotico DG, Locker J, Kalpana GV, and Mani S (2007) Inhibition of drug metabolism by blocking the activation of nuclear receptors by ketoconazole. *Oncogene* 26:258–268.

Ishida T and Kiwada H (2008) Accelerated blood clearance (ABC) phenomenon upon repeated injection of PEGylated liposomes. *Int J Pharm* 354:56–62.

Kanno Y, Tanuma N, Yazawa S, Zhao S, Inaba M, Nakamura S, Nemoto K, and Inouye Y (2016) Differences in gene regulation by dual ligands of nuclear receptors constitutive androstane receptor (CAR) and pregnane X receptor (PXR) in HepG2 cells stably expressing CAR/PXR. *Drug Metab Dispos* 44:1158–1163.

Kawana K, Ikuta T, Kobayashi Y, Gotoh O, Takeda K, and Kawajiri K (2003) Molecular mechanism of nuclear translocation of an orphan nuclear receptor, SXR. *Mol Pharmacol* 63:524–531.

Kliewer SA, Goodwin B, and Willson TM (2002) The nuclear pregnane X receptor: a key regulator of xenobiotic metabolism. *Endocr Rev* 23:687–702.

Kliewer SA, Moore JT, Wade L, Staudinger JL, Watson MA, Jones SA, McKee DD, Oliver BB, Willson TM, Zetterström RH, et al. (1998) An orphan nuclear receptor activated by pregnanes defines a novel steroid signaling pathway. *Cell* 92:73–82.

Lehmann JM, McKee DD, Watson MA, Willson TM, Moore JT, and Kliewer SA (1998) The human orphan nuclear receptor PXR is activated by compounds that regulate CYP3A4 gene expression and cause drug interactions. *J Clin Invest* 102:1016–1023.

Li Y, Liu R, Yang J, Shi Y, Ma G, Zhang Z, and Zhang X (2015) Enhanced retention and anti-tumor efficacy of liposomes by changing their cellular uptake and pharmacokinetics behavior. *Biomaterials* 41:1–14.

Ma X, Cheung C, Krausz KW, Shah YM, Wang T, Idle JR, and Gonzalez FJ (2008) A double transgenic mouse model expressing human pregnane X receptor and cytochrome P450 3A4. *Drug Metab Dispos* 36:2506–2512.

Maglich J, Sluder A, Guan X, Shi Y, McKee D, Carrick K, Kamdar K, Willson T, and Moore J (2001) Comparison of complete nuclear receptor sets from the human, Caenorhabditis elegans and Drosophila genomes. *Genome Biol* 2:research0029.1.

Mangelsdorf DJ and Evans RM (1995) The RXR heterodimers and orphan receptors. *Cell* 83:841–850.

Moore LB, Parks DJ, Jones SA, Bledsoe RK, Consler TG, Stimmel JB, Goodwin B, Liddle C, Blanchard SG, Willson TM, et al. (2000) Orphan nuclear receptors constitutive androstane receptor and pregnane X receptor share xenobiotic and steroid ligands. *J Biol Chem* 275:15122–15127.

Nagy L, Kao HY, Chakravarti D, Lin RJ, Hassig CA, Ayer DE, Schreiber SL, and Evans RM (1997) Nuclear receptor repression mediated by a complex containing SMRT, mSin3A, and histone deacetylase. *Cell* 89:373–380.

Papahadjopoulos D, Allen TM, Gabizon A, Mayhew E, Matthay K, Huang SK, Lee KD, Woodle MC, Lasic DD, Redemann C, et al. (1991) Sterically stabilized liposomes: improvements in pharmacokinetics and antitumor therapeutic efficacy. *Proc Natl Acad Sci USA* 88:11460–11464.

Pascussi JM, Gerbal-Chaloin S, Duret C, Daujat-Chavanieu M, Vilarem MJ, and Maurel P (2008) The tangle of nuclear receptors that controls xenobiotic metabolism and transport: crosstalk and consequences. *Annu Rev Pharmacol Toxicol* 48:1–32.

Pavek P (2016) Pregnane X receptor (PXR)-mediated gene repression and cross-talk of PXR with other nuclear receptors via coactivator interactions. *Front Pharmacol* 7:456.

Rysä J, Buler M, Savolainen MJ, Ruskoaho H, Hakkola J, and Hukkanen J (2013) Pregnane X receptor agonists impair postprandial glucose tolerance. *Clin Pharmacol Ther* 93:556–563.

Scheer N, Kapelyukh Y, Rode A, Oswald S, Busch D, McLaughlin LA, Lin D, Henderson CJ, and Wolf CR (2015) Defining human pathways of drug metabolism in vivo through the development of a multiple humanized mouse model. *Drug Metab Dispos* 43:1679–1690.

Shah YM, Ma X, Morimura K, Kim I, and Gonzalez FJ (2007) Pregnane X receptor activation ameliorates DSS-induced inflammatory bowel disease via inhibition of NF-kappaB target gene expression. *Am J Physiol Gastrointest Liver Physiol* 292:G1114–G1122.

Shi D, Yang D, and Yan B (2010) Dexamethasone transcriptionally increases the expression of the pregnane X receptor and synergistically enhances pyrethroid esfenvalerate in the induction of cytochrome P450 3A23. *Biochem Pharmacol* 80:1274–1283.

Sinz MW (2013) Evaluation of pregnane X receptor (PXR)-mediated CYP3A4 drug-drug interactions in drug development. *Drug Metab Rev* 45:3–14.

Smutny T, Mani S, and Pavek P (2013) Post-translational and post-transcriptional modifications of pregnane X receptor (PXR) in regulation of the cytochrome P450 superfamily. *Curr Drug Metab* 14:1059–1069.

Squires EJ, Sueyoshi T, and Negishi M (2004) Cytoplasmic localization of pregnane X receptor and ligand-dependent nuclear translocation in mouse liver. *J Biol Chem* 279:49307–49314.

Suk JS, Xu Q, Kim N, Hanes J, and Ensign LM (2016) PEGylation as a strategy for improving nanoparticle-based drug and gene delivery. *Adv Drug Deliv Rev* 99 (Pt A):28–51.

Tojima H, Kakizaki S, Yamazaki Y, Takizawa D, Horiguchi N, Sato K, and Mori M (2012) Ligand dependent hepatic gene expression profiles of nuclear receptors CAR and PXR. *Toxicol Lett* 212:288–297.

Vaclavikova R, Soucek P, Svobodova L, Anzenbacher P, Simek P, Guengerich FP, and Gut I (2004) Different in vitro metabolism of paclitaxel and docetaxel in humans, rats, pigs, and minipigs. *Drug Metab Dispos* 32:666–674.

Wang F, Wu Y, Zhang J, Wang H, Xie X, Ye X, Peng D, and Chen W (2019) Induction of cytochrome P450 involved in the accelerated blood clearance phenomenon induced by PEGylated liposomes in vivo. *Drug Metab Dispos* 47:364–376.

Willson TM and Kliewer SA (2002) PXR, CAR and drug metabolism. *Nat Rev Drug Discov* 1:259–266.

Wolf KK, Wood SG, Hunt JA, Walton-Strong BW, Yasuda K, Lan L, Duan SX, Hao Q, Wrighton SA, Jeffery EH, et al. (2005) Role of the nuclear receptor pregnane X receptor in acetaminophen hepatotoxicity. *Drug Metab Dispos* 33:1827–1836.

Xu C, Li CY, and Kong AN (2005) Induction of phase I, II and III drug metabolism/transport by xenobiotics. *Arch Pharm Res* 28:249–268.

Xu H, Ye F, Hu M, Yin P, Zhang W, Li Y, Yu X, and Deng Y (2015) Influence of phospholipid types and animal models on the accelerated blood clearance phenomenon of PEGylated liposomes upon repeated injection. *Drug Deliv* 22:598–607.

Address correspondence to: Dr. Weidong Chen, School of Pharmaceutical Sciences, Anhui University of Chinese Medicine, 1 Qianjiang Road, Hefei 230012, Anhui, China. E-mail: wdchen@ahtcm.edu.cn; or Dr. Daiyin Peng, School of Pharmaceutical Sciences, Anhui University of Chinese Medicine, 1 Qianjiang Road, Hefei 230012, Anhui, China. E-mail: pengdy@ahtcm.edu.cn

SUPPLEMENTARY MATERIAL

Activation of PXR-Cytochrome P450s axis: A Possible Reason for the Enhanced Accelerated Blood Clearance Phenomenon of PEGylated Liposomes *in vivo*

Fengling Wang, Huihui Wang, Yifan Wu, Lei Wang, Ling Zhang, Xi Ye, Daiyin Peng, Weidong Chen

Institute of Drug Metabolism, School of Pharmaceutical Sciences, Anhui University of Chinese Medicine, Hefei 230012, Anhui, China (F.W., H.W., Y.W., L.W., L.Z., D.P., W.C.); Department of Pharmacy, The Second People's Hospital of Hefei, Hefei 230011, Anhui, China (F.W., X.Y.); Anhui Province Key Laboratory of Chinese Medicinal Formula, Hefei 230012, China (L.W., L.Z., D.P., W.C.); Synergetic Innovation Center of Anhui Authentic Chinese Medicine Quality Improvement, Hefei 230012, China (D.P., W.C.); Institute of Pharmaceutics, School of Pharmaceutical Sciences, Anhui University of Chinese Medicine, Hefei 230012, Anhui, China (W.C.)

Running Title Page

PXR-CYPs axis involved in the ABC phenomenon

Corresponding author: Weidong Chen

Co-corresponding author: Daiyin Peng

Address: School of Pharmaceutical Sciences, Anhui University of Chinese Medicine, 1 Qianjiang Road, Hefei 230012, Anhui, China; E-mail: wdchen@ahtcm.edu.cn (Weidong Chen) and pengdy@ahtcm.edu.cn (Daiyin Peng); Telephone: +86 0551 68129123; Fax: +86 0551 68129123

Fengling Wang and Huihui Wang contribute equally to the manuscript.

Supplementary methods

Preparation for blood and tissues of interest samples

The samples preparation for blood and tissues of interest (liver and spleen) are the same as our previous studies. In brief, under isoflurane anesthesia, approximate 0.3 mL intraorbital blood samples were harvested in pre-heparinized tubes before (blank blood) and after intravenous administration of the preplanned time points (0.167, 0.5, 1, 2, 4, 6, 8, 10, and 12 h). After centrifuging the samples at 3000 rpm for 10 min, and 100 μL plasma fractions were obtained and kept at -80°C until further liquid chromatography-tandem mass spectrometry (LC-MS/MS) analysis.

Liver and spleen were rapidly removed and collected after the last blood sample was obtained at 12 h, and one piece of liver and spleen was excised for biodistribution analysis. A piece of liver was fixed with 4% paraformaldehyde for immunochemical staining. The rest of liver was then rinsed in ice-cold 0.9% NaCl, and a small piece of hepatic tissue was placed into a RNase-free Eppendorf tube for the measurement of mRNA. The remaining liver and spleen tissues were quickly frozen in liquid nitrogen and kept at -80°C until additional analysis.

The DTX levels in blood and tissue samples were measured using a previously developed detection method. Briefly, 3-fold volume of methyl tert-butyl ether with 25 ng/mL paclitaxel (internal standard, IS) was added in plasma or tissue homogenates followed by swirling for 3 min. The supernatant was separated by centrifuging for 5 min at high speed (12,000 rpm) and low temperature (4°C). Subsequently, the samples evaporated to dryness under nitrogen and reconstituted with methanol for LC-MS/MS analysis.

An Agilent 1260 series HPLC system (Agilent Technologies Inc., Shanghai, China) coupled

with a G6460H MS/MS spectrometer (Agilent Technologies Inc., Waldbronn, Germany) was applied to chromatographic analysis. 5 μL sample solution were injected into LC vial. Analytes were separated on a DIKMA® Leapsil C_{18} column (3.0×50, 2.7 μm) with a run time of 4.0 min at a constant flow rate of 0.4 mL/min maintained at 30°C.

The LC mobile phase for the detection of DTX was a mixture of methanol and aqueous phase 1 mM ammonium formate solution (Merck, Darmstadt, Germany), adjusted to pH 6.5 with formic acid (45:55, v/v, Merck, Darmstadt, Germany) with an injection volume of 5 μL. Quantitation was operated in the positive electrospray ionization mode (ESI^+). In the multiple reaction monitoring (MRM) mode, two optimal MRM transitions per analyte were monitored for DTX (m/z 830.4→549.3 with a collision energy (CE) of 15 V and a fragment voltage of 135 V) and for paclitaxel (IS) (m/z 876.8→308.5 with a CE of 18 V and a fragment voltage of 115 V), respectively. Under the LC-MS/MS conditions described above, DTX and IS were eluted at 1.986 min and 1.785 min, respectively. No significant effect of endogenous compounds on the analytes in the typical chromatograms. The recovery of drug in plasma and tissue samples were >92% and the standard curves with *r* value of more than 0.995 (weighting factor of $1/x^2$).

RT-qPCR analysis

Total RNA extraction and cDNA synthesis as well as RT-qPCR were followed as earlier reports (Rio et al., 2010; Doak and Zaïr, 2012). Total RNA was isolated from liver samples with TRIzol reagent (Life Technologies Inc., Carlsbad, USA) following the manufacturer's manual. The quality and quantity of the RNA were performed on a SoftMax® Pro 5 Multiscan Spectrum (Molecular Devices, Silicon Valley, USA) with the value of absorbance of each RNA sample (A_{260} nm/A_{280} nm) was 1.8 and 2.0. A StepOne Plus PCR System (Applied Biosystems, CA, USA) with

SYBR Green PCR kit (QIAGEN, Frankfurt, Germany) was used to run PCR samples as reported in detail previously, using the primers (Sangon Biotech Co., Ltd., Shanghai, China) given in Table S1. Running conditions was as follows: initial denaturation (95°C, 10 min) for one cycle, followed by denaturation (95°C, 15 s) for 40 cycles and annealing (60°C, 60 s). Last, specificity of the product was confirmed by melting curve analysis. Relative quantification analysis of target gene was calculated using the CT ($2^{-\Delta\Delta CT}$) method and normalized relative to stable reference gene β-actin (a housekeeping gene) (Livak and Schmittgen, 2001). Each result of RT-qPCR reaction was reproducible and reliable in three times.

**Supplementary Table S1** Primer sequences for SYBR green-based qPCR used in this study

| Target gene	Forward primer	Reverse primer
CYP1A2	5'-CATCTTTGGAGCTGGATTTG-3'	5'-CCATTCAGGAGGTGTCC-3'
CYP2C6	5'-TCAGCAGGAAAACGGATGTG-3'	5'-AATCGTGGTCAGGAATAA AAA TAACTC-3'
CYP3A1	5'-TGCCATCACGGACACAGA-3'	5'-ATCTCTTCCACTCCTCATCCTTAG-3'
PXR	5'-GAGGTCTTCAAATCTGCCGTGTA-3'	5'-CGGTGGAGCCTCAATCTTTTC-3'
CAR	5'-GTGTCTAAATGTTGGCATGAGGA-3'	5'-GTGATGGCTGAACAGGTAGGC-3'
β-actin	5'-GCCCAGAGCAAGACAGGTAT-3'	5'-GGCCATCTCCTGCTCGAAGT-3'

Western blotting analysis

To determine total protein expression, rat liver tissues (~50 mg) were homogenized and lysed with 1mL RIPA lysis buffer for 30 min on ice. Protein concentration was detected by BCA protein assay method. After denaturation with 5×SDS-PAGE loading buffer at 95°C for 10 min, total protein (20~30 μg) from lysates was separated by 12% SDS-PAGE and transferred onto an NC

membrane. After blocking with 5% non-fat milk in Tris buffered saline containing 0.05% Tween-20 (TBS-T), blots were incubated with appropriate dilutions of the primary anti-CYP3A1, anti-CYP2C6, anti-CYP1A2, anti-PXR, anti-CAR and anti-GAPDH (as internal reference) antibodies at 4°C for 12 h. Correspondingly, horseradish peroxidase-conjugated secondary anti-mouse or -rabbit antibodies (in 10 mL 0.05% TBS-T with 1:10000 dilution) were added to the membrane and incubated at room temperature for 2 h. After washing with 0.05% TBS-T, protein bands were visualized using the ECL detection reagents according to the defined operation and the relative intensity of protein expression was normalized to GAPDH. The experiments for determination of all protein expression were performed in triplicates and the results were reproducible. Alpha Chemiluminescent gel imaging system FluorChem FC3 (ProteinSimple, silicon valley, USA) was using for scanning protein bands, which were quantified by an ImageJ software (version 1.45S, NIH, USA).
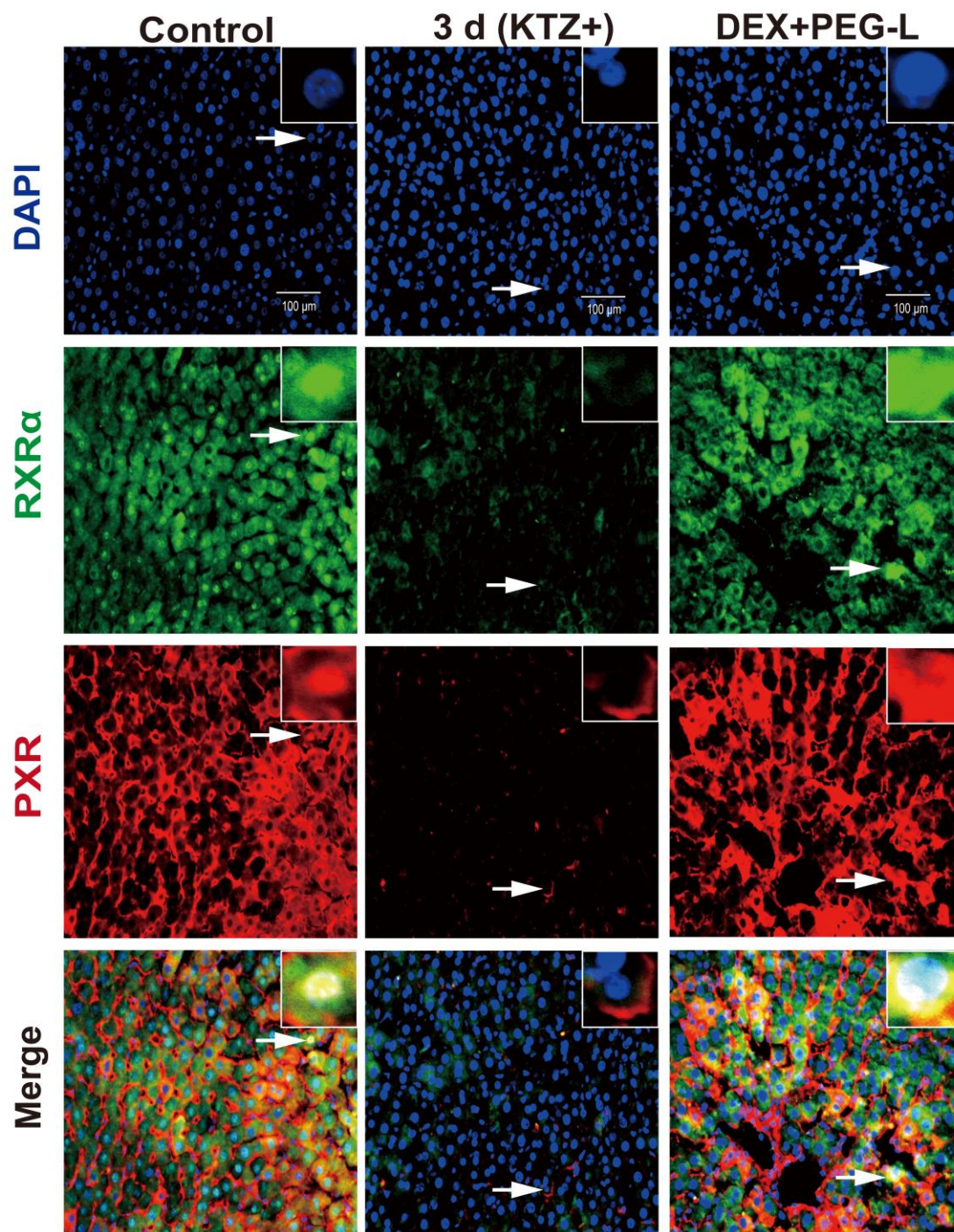
Supplementary Figures:
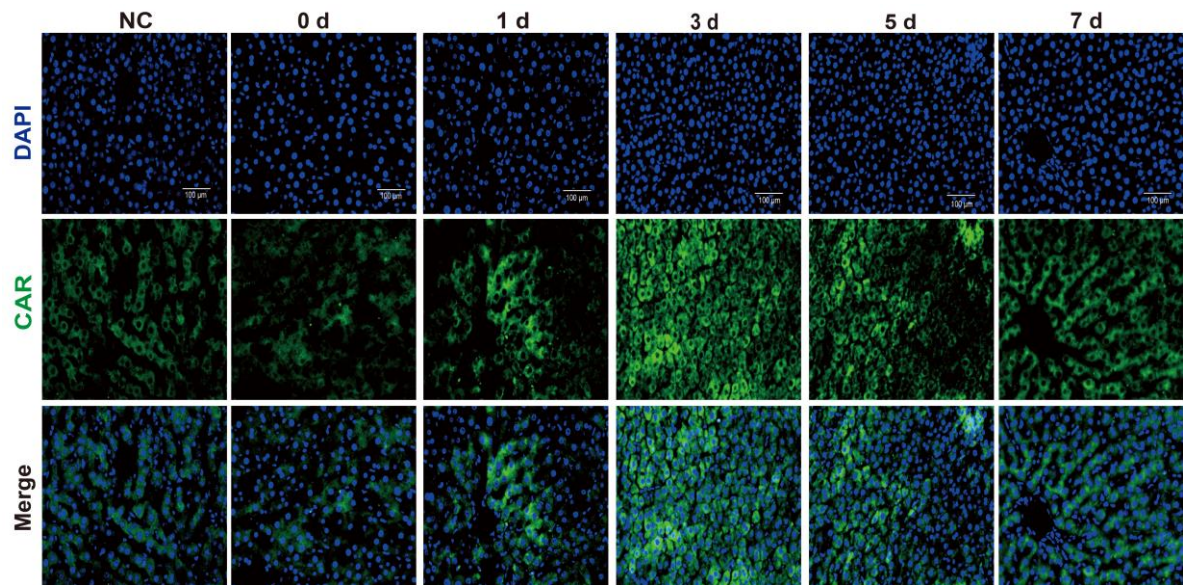
Supplementary Fig. S1. Immunofluorescence staining showed the location of hepatic CAR protein in hepatocytes (n=3). CAR shown in green and nuclei were stained with DAPI (blue). 0 d, 1 d, 3 d, 5 d, and 7 d indicate rats received repeated injection of PEG-L with different time intervals including 0, 1, 3, 5, and 7 days. Normal control group (NC) was injected with a single injection of equal volume of PBS. Scale bar: 100μm. PEG-L, PEGylated liposomes.
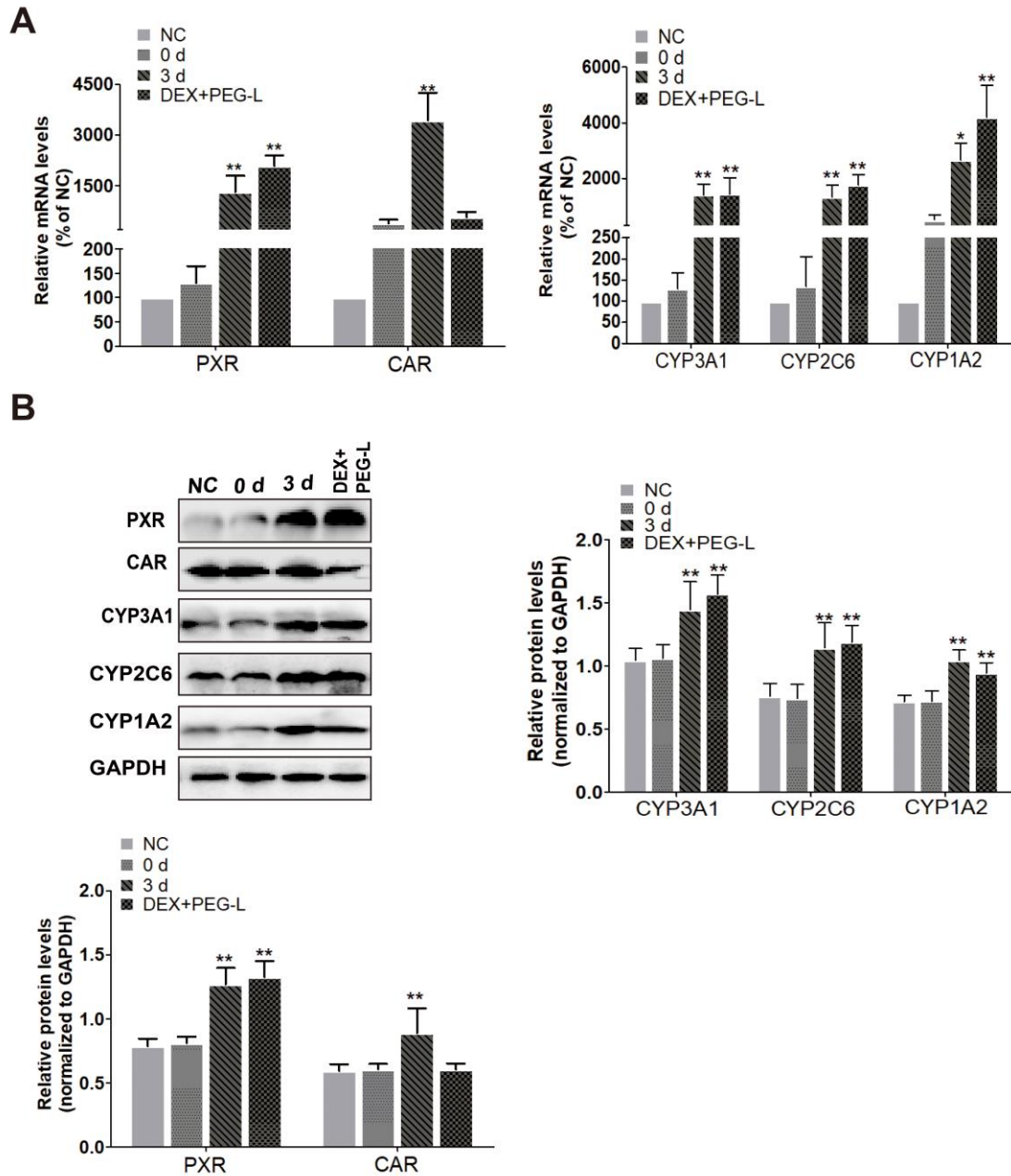
Supplementary Fig. S2. Effect of the presence of PXR inducer on the expression of hepatic PXR, CAR and CYPs. (A) RT-qPCR analysis the relative mRNA transcript levels of hepatic PXR, CAR and CYPs. Using β-actin as an endogenous reference gene, the values were normalized to the control group and fold change was calculated by $2^{-\Delta\Delta CT}$ method. (B) The relative protein expression of hepatic PXR, CAR and CYPs were analyzed by western blotting. Bar graphs show quantitative evaluation of PXR, CAR and CYPs bands by densitometry from triplicate

independent experiments. Each band density was evaluated by ImageJ software and these data were calculated as percentage compared to GAPDH. 0 d and 3 d indicate a single injection and repeated injections of PEG-L in rats with 3 days interval, respectively. DEX+ PEG-L presents intraperitoneally pretreated with DEX for 3 consecutive days combined with a subsequent injection of PEG-DTX-L (0.05 μmol/kg). Normal control group (NC) was injected with a single injection of equal volume PBS. Data are presented as the mean $\pm$ SD (n=5 ~ 6). $^{*}P < 0.05$, $^{**}P < 0.01$ compared with 0 d group.

Supplementary Fig. S3. Response of the nuclear translocation of hepatic PXR and RXRα proteins in rats exposed to the coadministration of DEX with an injection of PEG-DTX-L (n=3). PXR and RXRα are shown in red and green, respectively, and nuclei were stained with DAPI (blue). Control rats received repeated injection of PEG-L with 3-day interval; group 3 d (KTZ+) indicates the samples obtained from our previous studies that rats were pretreated with oral

administration 100 mg/kg/day of KTZ for 7 consecutive days combined with repeated injection of

PEG-L with 3-day interval; group DEX+ PEG-L has been mentioned in Table 1. Scale bar: 100μm.

PEG-L, PEGylated liposomes; DEX, dexamethasone; KTZ, ketoconazole.

References

Doak S and Zaïr Z (2012) Real-time reverse-transcription polymerase chain reaction: technical

considerations for gene expression analysis. Methods Mol Biol 817:251-270.

Livak K and Schmittgen T (2001) Analysis of relative gene expression data using real-time

quantitative PCR and the 2(-Delta Delta C(T)) Method. Methods 25:402-408..

Rio D, Ares M, Hannon G, and Nilsen T (2010) Purification of RNA using TRIzol (TRI reagent).

Cold Spring Harb Protoc 2010:pdb.prot5439.